Environ. Sci. Technol. **2003**, *37,* 4182−4189

Comparison of Arsenic(V) and Arsenic(III) Sorption onto Iron Oxide Minerals: Implications for Arsenic Mobility

SUVASIS DIXIT AND JANET G. HERING*

California Institute of Technology, 1200 East California Boulevard, Environmental Science and Engineering (138-78), Pasadena, California 91125

Arsenic derived from natural sources occurs in groundwater in many countries, affecting the health of millions of people. The combined effects of As(V) reduction and diagenesis of iron oxide minerals on arsenic mobility are investigated in this study by comparing As(V) and As(III) sorption onto amorphous iron oxide (HFO), goethite, and magnetite at varying solution compositions. Experimental data are modeled with a diffuse double layer surface complexation model, and the extracted model parameters are used to examine the consistency of our results with those previously reported. Sorption of As(V) onto HFO and goethite is more favorable than that of As(III) below pH 5−6, whereas, above pH 7−8, As(III) has a higher affinity for the solids. The pH at which As(V) and As(III) are equally sorbed depends on the solid-to-solution ratio and type and specific surface area of the minerals and is shifted to lower pH values in the presence of phosphate, which competes for sorption sites. The sorption data indicate that, under most of the chemical conditions investigated in this study, reduction of As(V) in the presence of HFO or goethite would have only minor effects on or even decrease its mobility in the environment at near-neutral pH conditions. As(V) and As(III) sorption isotherms indicate similar surface site densities on the three oxides. Intrinsic surface complexation constants for As(V) are higher for goethite than HFO, whereas As(III) binding is similar for both of these oxides and also for magnetite. However, decrease in specific surface area and hence sorption site density that accompanies transformation of amorphous iron oxides to more crystalline phases could increase arsenic mobility.

Introduction

Arsenic has been found to occur naturally at concentrations exceeding 10 ppb or 0.13 μM, the United States and WHO drinking water standards (*1, 2*), in groundwater in many countries and has been implicated in human disease and mortality, most notably in Taiwan (*3*), India (*4*), Chile (*5*), and Bangladesh (*6, 7*). These occurrences of arsenic have been distinguished based on the prevailing redox conditions in the aquifers (*7*). Under oxidizing conditions, As(V) is predominant and is mobilized at high pH (*7*). In reducing environments, arsenic occurs mostly as As(III). Several mechanisms (singly or in combination) have been invoked to explain arsenic mobility. These include microbial reduction of As(V), reductive dissolution of iron oxyhydroxide phases, and competition of solutes for sorption sites on iron oxides (*6*−*11*). A close coupling between the biogeochemical cycles of iron and arsenic in both oxidizing and reducing environments has been well established (for reviews see refs *7, 12*−*14*).

Numerous studies have quantified and modeled As(V) and As(III) sorption onto amorphous iron oxides, goethite, lepidocrocite, and hematite (*15*−*26*). Both As(V) and As(III) sorb strongly to iron oxide; however, the sorption behavior of arsenic is dependent on its oxidation state and the mineralogy of the iron oxides. Competition between arsenic and other sorbates (such as phosphate, silicic acid, and bicarbonate) has also been studied (*22*−*26*). Phosphate, whose concentrations in groundwater can exceed those of arsenic, is particularly effective at competing with arsenate for sorption sites on iron oxide minerals (*24*−*26*). A positive correlation has been found between arsenic and phosphate in groundwater in Bangladesh (*27*). In contrast, silicic acid (although present at concentrations 10 times higher than phosphate) shows no correlation with arsenic levels of the well waters (van Geen, personal communication).

Iron oxide minerals often form in natural waters and sediments at oxic−anoxic boundaries. The solids formed initially are poorly crystalline and have high specific surface area but, over time, undergo transformation to more crystalline forms, such as goethite or hematite. The time scale of these transformations varies depending on temperature, pH, and the presence of other co-occurring solutes (*28*−*30*). In natural sediments, both crystalline and amorphous iron oxide minerals can coexist; crystalline solids can be 2 to >10 times more abundant (based on Fe content) than amorphous solids (*31*). Recent studies have also shown that amorphous iron oxides are transformed to magnetite during reductive dissolution (*32*−*33*). Therefore, the mobilization of arsenic during the transformation of iron oxides will depend on the relative affinity of the original and transformed minerals for the arsenic species.

The objectives of this study are to investigate the conditions under which reduction of arsenate would favor its mobilization and compare the relative affinity of arsenic for different iron oxide minerals. Previous studies quantifying arsenic sorption onto iron oxide minerals have focused either on one arsenic species or one type of solid. Therefore, the combined effect of arsenate reduction and diagenesis of iron minerals on arsenic mobility remains unclear. In this study, we compare the sorption of As(V) and As(III) onto HFO and goethite at different total arsenic concentrations and in the presence of phosphate. These results show that the effect of As(V) reduction on arsenic mobility will be strongly dependent on solution composition. Arsenic mobility during early diagenesis is evaluated by comparing the affinity and sorption densities of HFO, goethite, and (for the first time) magnetite for As(III). The different iron oxide minerals are found to exhibit, on a surface area normalized basis, similar sorption densities for arsenite and also similar binding constants.

Materials and Methods

Materials. All chemicals were reagent grade and used without further purification. Solutions were prepared with Milli-Q (18 MΩ-cm) water. Plastic volumetric flasks and reaction vessels (Polypropylene) were cleaned with 1% HNO_3 and rinsed several times with deionized water before use. As(V) stock solution was prepared from reagent grade Na_2HAsO_4·

* Corresponding author phone: (626)395-3644; fax: (626)395-2940; e-mail: jhering@caltech.edu.

10.1021/es030309t CCC: $25.00
Published on Web 08/13/2003

TABLE 1. Material Properties and Experimental Conditions[a]

	HFO	goethite	magnetite
specific surface area[b] ($m^2\ g^{-1}$)	600[c]	54	90
solid concentration ($g\ L^{-1}$)	0.03	0.5	0.5
equilibration time (h)	4	24	24
total As concentration (μM)	10−100	10−100	50−150
As-to-Fe ratio ($\times 10^{-3}$)	30−300	2−18	8−23
sorption density[d]			
As (V)			
mol As per mol Fe	0.24	0.016	
sites per nm^2	2.6	2.0	
As (III)			
mol As per mol Fe	0.31	0.016	0.025
sites per nm^2	3.5	2.0	2.2

[a] All experiments conducted at room temperature (23 ± 0.4 °C) with 0.01 M $NaClO_4$ background electrolyte medium. [b] Measured by N_2 BET. [c] Assumed value (*36*). [d] Obtained from sorption isotherm.

$7H_2O$ (Sigma) and As(III) stock from $NaAsO_2$ (J. T. Baker). Phosphate stock solution was prepared from $NaH_2PO_4 \cdot H_2O$ (Merck).

Mineral Sorbents. Sorption experiments were conducted with three iron oxides: HFO, goethite, and magnetite. HFO was synthesized by the method of Schwertmann and Cornell (*34*), as modified by Wilkie and Hering (*20*). Fresh HFO was prepared each day for the experiments. Goethite was prepared by mixing 180 mL of 5 M KOH with 100 mL of 1 M $Fe(NO_3)_3 \cdot 9H_2O$ (*34*). The suspension was diluted to 2 L and aged for 60 h at 70 °C. After the synthesis of the minerals, suspensions were washed repeatedly with deionized water and freeze-dried. Both oxides were prepared under ambient atmospheric conditions.

Magnetite was synthesized by slow addition of a mixture of ferrous and ferric chloride solutions (10 mL of 2 M $FeCl_2$ added to 40 mL of 1 M $FeCl_3$ solution) to 400 mL of 0.9 M NH_3 solution (*35*). Both the ammonia solution and aqueous Fe solutions were purged with N_2 gas prior to their use and purging was continued during the mineral synthesis. The supernatant was then decanted, and solids were washed five times in the reaction vessel with N_2-purged water. Solid suspensions were then transferred to 250 mL centrifuged bottles and washed repeatedly with deionized water. The solids were then freeze-dried.

The multipoint BET surface areas of the solids determined by N_2 adsorption using a Gemini 2360 surface area analyzer (Micromeritics) are given in Table 1. For HFO, a specific surface area of 600 $m^2\ g^{-1}$ is assumed (*36*). The identity of the solids (except HFO) was confirmed with a Scintag Pad V X-ray diffractometer using a copper X-ray source.

Arsenic Adsorption Edges. All the experiments were performed with a background electrolyte of 0.01 M $NaClO_4$. Sorption of As(III) and As(V) onto iron oxides was initiated by the addition of solid suspensions at different pH values to arsenic stock solutions. The pH of the resulting suspensions drifted (by up to 1−2 pH units at near neutral pH) in the first 5−10 min and then stabilized. The final pH, measured at the end of the experiments, is reported. Suspensions were continuously mixed using an end-over-end shaker. Experimental conditions are summarized in Table 1. The solid concentrations chosen correspond to similar total concentrations of surface sites for HFO and goethite and about 2-fold higher surface site concentrations for magnetite. Equilibration times for experiments with HFO and goethite were based on previous studies (*18, 16*), and determined for magnetite in preliminary experiments. After the desired reaction time, the suspensions were centrifuged, and the supernatant was filtered through 0.2 μm filters (Nalgene, cellulose acetate) and analyzed for arsenic. The amount of arsenic sorbed to the solids was calculated by difference. In experiments with HFO, the solid concentration was verified by dissolving the suspension in 1% HNO_3 and analyzing for total iron. Sorption experiments with HFO and goethite were conducted in open atmospheric conditions. A few experiments performed under N_2 in an anaerobic chamber (Vacuum Atmospheres Dri-Lab HE-63-P) did not reveal any difference in the sorption edges. All sorption experiments with magnetite were conducted inside the anaerobic chamber.

Sorption Isotherms. Sorption isotherms on the iron oxides were conducted to estimate the maximum sorption density. The experiments were performed at pH 4.0 ± 0.1 for As(V) and at pH 8.0 ± 0.2 for As(III), corresponding to the pH values of maximum sorption of the arsenic species. The pH of the suspensions was adjusted with $HClO_4$ and NaOH during the experiment.

Arsenic Sorption in the Presence of Phosphate. The influence of phosphate on arsenic sorption was studied by simultaneously adding arsenic and phosphate stock solutions to sorbent suspensions prepared at different pH values. Both the phosphate and arsenic concentrations of filtered solutions and pH were measured at the end of the experiment.

Analytical Methods. The pH of the solutions was measured using an Orion model 720A pH meter, calibrated using commercial pH 4.0, 7.0, and 10.0 buffers. Filtered solutions from sorption experiments were acidified with 1% HNO_3 and analyzed for total arsenic, phosphorus, and iron by ICP-MS. The relative standard deviation of these measurements was always better than 5%.

Surface Complexation Model. A surface complexation model with the diffuse double layer (DDL) model for electrostatics was used to describe the arsenic sorption edges (*36*). Constants for protonation of the surface hydroxyl groups and aqueous species were taken from previous studies (Table 2). The stoichiometries of the surface complexes used to fit sorption data are listed in Table 2. Similar surface complexes have been used in previous studies (*19, 24, 26*). The computer program FITEQL (*40*) was used to obtain the intrinsic As(III) and As(V) surface complexation constants. The surface site densities were set to values obtained from sorption isotherms (Table 1), and only the surface complexation constants were optimized. Model predictions with fixed site densities and complexation constants were performed using $MINEQL^+$ (*37*). For both fitting and predictions, activity coefficients of aqueous species were calculated using the Davies equation.

Results and Discussion

Arsenate Sorption Edges on HFO and Goethite. Sorption of arsenate on HFO and goethite for total arsenate concentrations ranging from 10 to 100 μM is shown in Figure 1. In the pH range of the experiments, arsenate sorption on both the solids decreases with increasing pH (Figure 1).

At pH 4.0, the amount of As(V) sorbed onto both HFO and goethite remains close to 100% for total As(V) concentrations below 50 μM but decreases to 65% (with HFO) or 70% (with goethite) at 100 μM total As(V). Substantially less As(V) is sorbed at higher pH values. At pH 10, the sorbed concentrations of As(V) on HFO converge to a value of about 300 $\mu mol\ g^{-1}$, corresponding to 70, 30, and 7% of the total As(V) concentrations of 10, 35, and 100 μM, respectively. With goethite, the sorbed As(V) concentrations at pH 10 show less convergence and correspond to 85, 40, and 25% of the total As(V) concentrations of 10, 50, and 100 μM, respectively. The higher maximum sorption densities observed with HFO (2,100 $\mu mol\ g^{-1}$) as compared to goethite (140 $\mu mol\ g^{-1}$) are consistent with similar densities of sorption sites per unit area for both the solids but a much greater specific surface area for HFO than goethite.

Similar trends have been observed in several previous studies. However, the sorbent and sorbate concentrations were higher by as much as 2 orders of magnitude in those

TABLE 2. Aqueous Protonation Constants and Intrinsic Surface Complexation Constants[a]

reaction	log K or β
Arsenate Protonation Constants[b]	
$AsO_4^{3-} + H^+ = HAsO_4^{2-}$	11.60
$AsO_4^{3-} + 2H^+ = H_2AsO_4^-$	18.35
$AsO_4^{3-} + 3H^+ = H_3AsO_4$	20.60
Arsenite Protonation Constants[b]	
$AsO_3^{3-} + H^+ = HAsO_3^{2-}$	13.41
$AsO_3^{3-} + 2H^+ = H_2AsO_3^-$	25.52
$AsO_3^{3-} + 3H^+ = H_3AsO_3$	34.74

intrinsic surface complexation constants	HFO	goethite	magnetite
$\equiv FeOH + H^+ = \equiv FeOH_2^+$	7.29[b]	7.47[c]	4.60[d]
$\equiv FeOH = \equiv FeO^- + H^+$	−8.93[b]	−9.51[c]	−8.20[d]
Arsenate Adsorption Constants[e]			
$\equiv FeOH + AsO_4^{3-} + 3H^+ = \equiv FeH_2AsO_4 + H_2O$	29.88	31.00	
$\equiv FeOH + AsO_4^{3-} + 2H^+ = \equiv FeHAsO_4^- + H_2O$	24.43	26.81	
$\equiv FeOH + AsO_4^{3-} + H^+ = \equiv FeAsO_4^{2-} + H_2O$	18.10	20.22	
Arsenite Adsorption Constants[e]			
$\equiv FeOH + AsO_3^{3-} + 3H^+ = \equiv FeH_2AsO_3 + H_2O$	38.76	39.93	38.41
$\equiv FeOH + AsO_3^{3-} + 2H^+ = \equiv FeHAsO_3^- + H_2O$	31.87	32.40	33.02

[a] $I = 0$ M, activity coefficients in MINEQL$^+$ are calculated using the Davies equation. [b] Reference *37*. [c] Reference *38*. [d] Reference *39*. [e] This study.

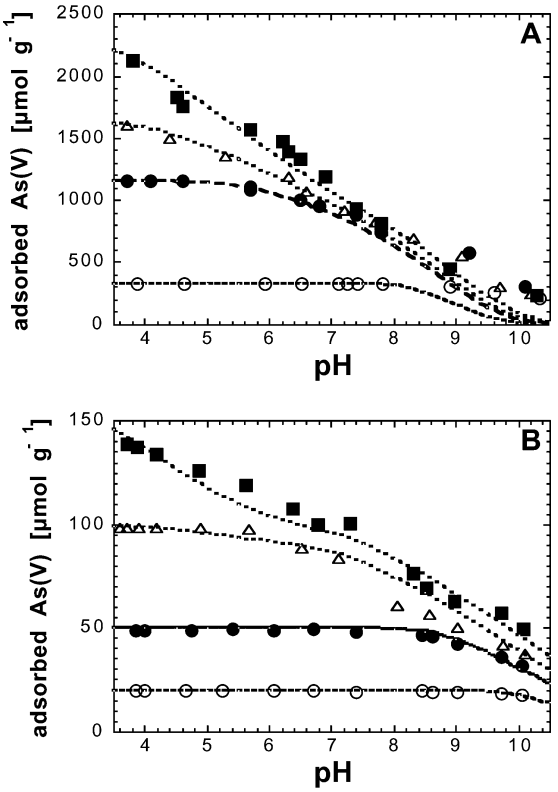

FIGURE 1. Arsenate sorption onto (a) amorphous iron oxide (HFO) and (b) goethite for total As(V) concentrations of (■) 100, (△) 50, (●) 35 for HFO and 25 for goethite, (○) 10 μM. Experimental conditions: 0.01 M $NaClO_4$; 0.03 g L^{-1} HFO or 0.5 g L^{-1} goethite. The lines represent surface complexation model fits based on parameters in Table 2.

studies (see Table 3). This complicates direct comparison with our results, and, thus, we use model parameters generated from our data to make this comparison in a later section.

Arsenite Sorption Edges on Iron Oxides. Arsenite sorption onto HFO, goethite, and magnetite as a function of pH from 4 to 10 are shown in Figure 2. Compared to arsenate, the effect of pH on sorption is much less pronounced. Sorption increases with increasing pH until a broad sorption maximum is observed, after which sorption decreases with further increases in pH. This pattern is most obvious with HFO for which the sorption maximum occurs between pH 6 and 9. With goethite, the sorption maximum is so broad that almost no pH dependence is observed. With magnetite, the extent of sorption increases gradually over almost the entire pH range examined.

As observed for As(V), the maximum extent of As(III) sorption decreases with increasing total As(III) concentration. With goethite, As(III) sorption exceeds 95% when the total As(III) concentration is below 25 μM. With HFO, however, As(III) sorption reached only 90% even at 10 μM total As(III). With 100 μM total As(III), the percent As(III) sorbed decreases to 60% for goethite (120 μmol g^{-1}) and 45% for HFO (1600 μmol g^{-1}). With both solids, the maximum sorption density for As(III) (at pH 8) is less than that for As(V) (at pH 4); this difference is less pronounced for goethite than HFO. With magnetite, 70% of the total As(III) concentration of 100 μM is sorbed at pH 9.0; the observed sorption density of 140 μmol g^{-1} is very similar to that of goethite.

Comparing Sorption Edges of Arsenate and Arsenite. Arsenate and arsenite sorption edges on HFO and goethite are compared in Figure 3. For both the solids, As(V) sorption is more favorable than As(III) at lower pH values, but the opposite is true at higher pH values. With HFO, the crossover pH (i.e., the pH value at which As(III) and As(V) are equally sorbed) is about 6.5 with 50 or 100 μM total As (Figure 3a) and 8.5 with 10 μM total As (Figure 4a). Similar observations have been made in a previous study with 2 g L^{-1} HFO and 0.534, 1.60, and 26.7 mM total As (*18*). At the two lower As concentrations, a crossover pH of 7.5 was observed. However, at 26.7 mM total As, As(III) was adsorbed to a greater extent than As(V) from pH 3 to 11. As we show later in the modeling section, this last data set is not consistent with our results.

With goethite, the crossover pH is about 6.0 with 100 μM total As and increases to 7.0 with 50 μM total As (Figure 3b) and to between pH 7.0 and 8.5 with 25 μM of total As (Figure 4b). Manning et al. (*16*) observed equal sorption of As(V) and As(III) at pH 5.0 in experiments with 2.5 g L^{-1} goethite and 267 μM total As. A crossover pH of around 6.0 was observed by Sun and Doner (*21*) using a goethite concentration of 5 g L^{-1} and 1.25 mM total As. These variations in crossover pH values may reflect, in part, differences in the total sorbate and sorbent concentrations used in the experiments.

TABLE 3. Summary of Experimental Conditions and Surface Complexation Model Parameters from Previous Studies

system (ref)	total As (μM)	total Fe (mM)	As/Fe ($\times 10^{-3}$)	site density[a]	electrostatic model[b]	surface species	diagnostic parameters[c]: sorption max. (μmol g^{-1})	diagnostic parameters[c]: $pH_{1/2\ max}$
As(V), goethite (*16*)	267	28	10				85 (105)	9.0 (9.0)
As(V), goethite (*21*)	1250	56	22				200 (230)	>9.5 (9.5)
As(V), HFO (*17*)[d]	0.67	0.05	13				100% sorption up to pH 7.0	
	1.33		27				100% sorption up to pH 6.0	
	3.34		67				100% sorption up to pH 5.0	
	6.67		133				1200 (1350)	6.5 (7.5)
	13.3		266				1400 (1800)	6.5 (7.0)
As(V), HFO (*20*)	1.33	0.05	27	0.20	DDL	$\equiv FeH_2AsO_4$ $\equiv FeHAsO_4^-$ $\equiv FeAsO_4^{3-}$	100% sorption up to pH 7.0	
As(V), HFO (*18*)	534	22.5	24				100% sorption up to pH 9.0	
	1600		71				100% sorption up to pH 7.5	
	26700		1189				3500 (2700)	8.0 (8.5)
As(V), HFO (*23*)	53	1	53	0.20	DDL	$\equiv FeH_2AsO_4$	100% sorption up to pH 8.0	
	110		110			$\equiv FeHAsO_4^-$	100% sorption up to pH 7.0	
	210		210			$\equiv FeAsO_4^{2-}$ $\equiv FeAsO_4^{3-}$	2100 (2025)	8.5 (7.5)

system (ref)	total As (μM)	total Fe (mM)	As/Fe ($\times 10^{-3}$)	site density[a]	electrostatic model[b]	surface species	diagnostic parameters[c]: sorption max. (μmol g^{-1})	diagnostic parameters[c]: max. % sorbed
As(III), goethite (*16*)	133	28	5	2.31	CCM	$\equiv Fe_2HAsO_3$	53 (52)	100 (99)
	267		10			$\equiv Fe_2AsO_3^-$	90 (100)	84 (94)
As(III), goethite (*21*)	1250	56	22				215 (225)	86 (90)
As(III), HFO (*17*)[d]	0.67	0.05	13				120 (95)	80 (63)
	1.33		27				220 (180)	74 (60)
	3.34		67				400 (395)	53 (53)
	6.67		133				480 (635)	32 (42)
	13.3		266				500 (910)	17 (30)
As(III), HFO (*20*)	1.33	0.05	27	0.2	DDL	$\equiv FeH_2AsO_3$	190 (180)	64 (60)
As(III), HFO (*18*)	534	22.5	24				267 (267)	100 (100)
	1600		71				800 (800)	100 (100)
	26700		1189				5800 (3400)	44 (26)
As(III), HFO (*23*)	53	1	53	0.2	DDL	$\equiv FeH_2AsO_3$ $\equiv FeHAsO_3^-$ $\equiv FeAsO_3^{2-}$	560 (560)	94 (94)

[a] Expressed in mol sites (mol Fe)$^{-1}$ for HFO and sites nm^{-2} for goethite. [b] Constant capacitance model (CCM), diffuse double layer (DDL). [c] Predicted values are shown in brackets (see text for details). [d] Data sets listed have been previously used to extract model parameters (*36*).

Effect of Phosphate. Phosphate sorbs strongly onto iron oxide minerals (*24*−*26*) and can therefore compete with arsenic for surface sites (Figure 4a,b). Sorption of both phosphate and arsenate onto iron oxides decreases with increasing pH (*26*). The presence of phosphate decreases the crossover pH from 8.5 (with HFO and 10 μM total As) or 8.0 (with goethite and 25 μM total As) in the absence of phosphate to about 7.5 (for HFO) or 7.0 (for goethite) with 100 μM total phosphate.

The fraction of arsenic bound to HFO is reduced substantially in the presence of phosphate. At pH 4.0, As(V) sorption is decreased from >95% to about 80% and As(III) sorption from 75% to undetectable (Figure 4a). These results are similar to those reported in a previous study in which, at an arsenic-to-phosphate ratio of 1:10, As(V) sorption decreased from 100 to 60% and As(III) sorption from >95% to about 50% at pH 4.0 (*25*).

Similar trends were observed with goethite. In the absence of phosphate, >90% of 25 μM total As is sorbed at pH 4.0 (Figure 4b). With 100 μM total phosphate, As(V) sorption decreases to 65% and As(III) sorption to 15%. The decrease in arsenate sorption in the presence of phosphate is similar to that observed in previous studies (*24*, *26*), but the effect on sorption of arsenite has not been previously reported. It should be noted that most competitive sorption studies (including this work) have been performed by simultaneous addition of the solutes to solid suspensions. Liu et al. (*41*) have shown that the order in which the sorbates are added to goethite suspensions can affect the extent of competition observed.

Sorption Isotherms on Iron Oxides. Arsenic sorption isotherms were obtained at pH 4.0 for arsenate and at pH 8.0 for arsenite (Figure 5). With HFO, the maximum sorption density is 3514 ± 157 μmol g^{-1} or 0.31 mol As (mol Fe)$^{-1}$ for As(III) and is 2675 ± 250 μM g^{-1} or 0.24 mol As (mol Fe)$^{-1}$ for As(V). With the specific surface area of HFO assumed to be 600 m^2 g^{-1} (*36*), these values correspond to site densities of 3.5 sites nm^{-2} for As(III) and 2.6 sites nm^{-2} for As(V).

The maximum sorption density for As(V) on HFO is similar to the value of 0.25 mol As (mol Fe)$^{-1}$ previously reported for both pH 4.6 and pH 8.0 (*18*, *42*). Pierce and Moore (*17*) reported biphasic behavior for As(V) sorption on HFO. At lower total As(V) concentrations, they reported surface saturation with a maximum sorption density of 0.14 mol As (mol Fe)$^{-1}$. However, a linear isotherm was observed at higher total As(V) concentrations with sorption densities reaching as much as 4 mol As (mol Fe)$^{-1}$. These levels are clearly inconsistent with sorption processes, which are inherently limited by the availability of surface sites (and are therefore not included in Table 3).

For As(III), there are substantial discrepancies in estimates of the maximum sorption density on HFO. In two studies,

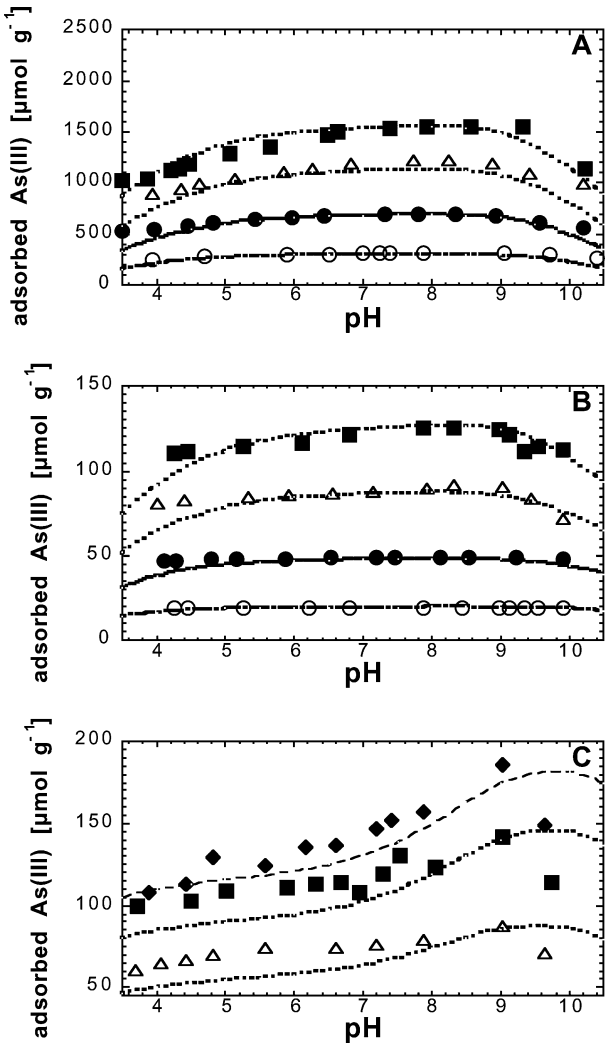

FIGURE 2. Arsenite sorption onto (a) HFO, (b) goethite, and (c) magnetite for total As(III) concentrations of (■) 100, (△) 50, (●) 25, (○) 10 μM and, for magnetite, (◆) 150 (■) 100, (△) 50 μM. Experimental conditions: 0.01 M $NaClO_4$; 0.03 g L^{-1} HFO or 0.5 g L^{-1} goethite or magnetite. The lines represent surface complexation model fits based on parameters in Table 2.

surface saturation was not observed even though surface coverages reached 0.60 mol As (mol Fe)$^{-1}$ (*18*) or 0.4 mol As (mol Fe)$^{-1}$ ((*43*), as referenced in ref *18*). Pierce and Moore (*17*) reported even higher sorption densities for As(III) on HFO, exceeding 4.5 mol As (mol Fe)$^{-1}$. However, at lower total As(III) concentrations, they reported a maximum sorption density of 0.046 mol As (mol Fe)$^{-1}$. This biphasic behavior was reported for both As(III) and As(V).

At the pH corresponding to the maximum sorption densities for As(III) and As(V), the sorption isotherms for As(III) and As(V) on goethite are quite similar (Figure 5b). The maximum sorption density is 173 ± 13 μmol g^{-1} or 0.016 mol As (mol Fe)$^{-1}$. The corresponding site density is calculated to be 2.0 sites nm^{-2}. This is 15% lower than the site density of 2.31 sites nm^{-2} used previously to model As(III) and As(V) sorption on goethite (*16, 24*). Potentiometric titration and metal adsorption studies on goethite also report similar site densities (summarized in ref *44*).

With magnetite, the maximum sorption density for As(III) is 332 ± 30 μmol g^{-1} or 0.025 mol As (mol Fe)$^{-1}$, which corresponds to a site density of 2.2 sites nm^{-2}. A site density of 5.2 sites nm^{-2} has been reported based on potentiometric titration of magnetite synthesized by the same procedure as used here (*45*). In comparison, a site density of 1.9 sites nm^{-2}

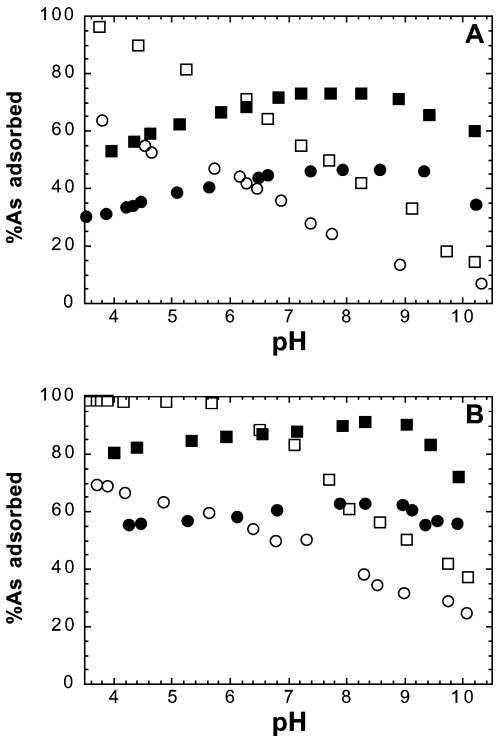

FIGURE 3. Comparison of As(V) and As(III) sorption edges on (a) HFO and (b) goethite. The total arsenic concentrations shown are 100 μM (circles) and 50 μM (squares). Open symbols represent As(V) and closed symbols As(III). Experimental conditions: 0.01 M $NaClO_4$; 0.03 g L^{-1} HFO or 0.5 g L^{-1} goethite. Data are taken from Figures 1 and 2.

is reported based on acid−base titration of a commercially available, low surface area magnetite (*39*).

In this study, similar values of site densities were obtained from arsenic sorption isotherms for HFO, goethite, and magnetite (Table 1). The As(III) sorption isotherms, obtained at pH 8.0, are normalized with respect to their sorption maxima and plotted in Figure 6. Despite the scatter in the data, it appears that the three iron oxides have similar affinities for As(III). This is further examined through surface complexation modeling in the following section.

Surface Complexation Modeling. Site densities, based on the maximum sorption densities for As(V) at pH 4.0 and As(III) at pH 8.0 for each solid (Figure 5, Table 1), were used in modeling the sorption data shown in Figures 1 and 2. For all the oxides, a consistent set of surface species was used to model sorption of either As(V) or As(III). Thus, it is informative to compare the values of intrinsic surface complexation constants for the various solids (Table 2). For all As(V) surface species, the constants for sorption onto goethite are higher (by 1.1−2.4 log units) than for HFO. For As(III), the surface complexation constant for the species $\equiv FeH_2AsO_3$ is similar for magnetite and HFO but that for the species $\equiv FeHAsO_3^-$ is higher for magnetite. Table 2 lists the surface species and the values of their surface complexation constants optimized for the data sets with the highest As-to-Fe ratios (since these data provide the greatest sensitivity of the model fits to the values of the constants). As seen in Figure 1, As(V) sorption onto HFO is underpredicted by the model for pH > 9.0. Better agreement between the model fits and the experimental data are obtained with goethite. For As(III), the model predicts a stronger pH dependence than observed with either HFO or goethite, but limited data are available to probe this discrepancy (Figure 2a,b). Disagreement between the data and model fits is greatest for As(III) sorption on magnetite; model fits underpredict

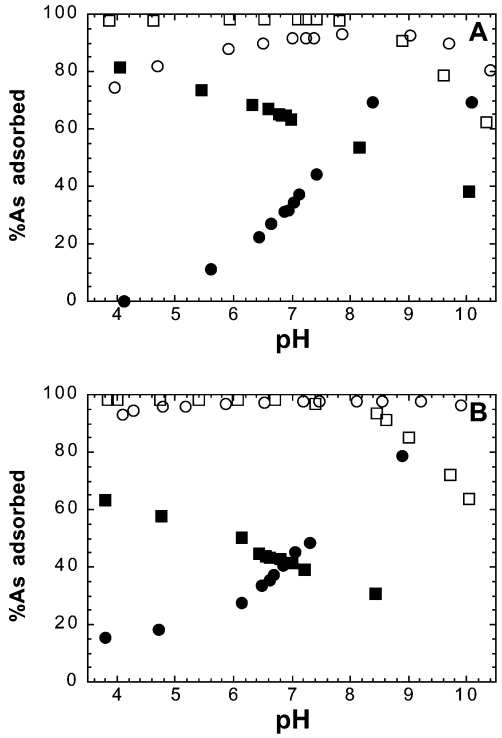

FIGURE 4. Comparison of As(V) and As(III) sorption edges on (a) HFO and (b) goethite in the presence (solid symbols) or absence (open symbols) of phosphate; As(V) (squares) and As(III) (circles). Total arsenic concentrations are 10 and 25 μM for HFO and goethite, respectively. Total phosphate concentration is 100 μM. Experimental conditions: 0.01 M $NaClO_4$; 0.03 g L^{-1} HFO or 0.5 g L^{-1} goethite.

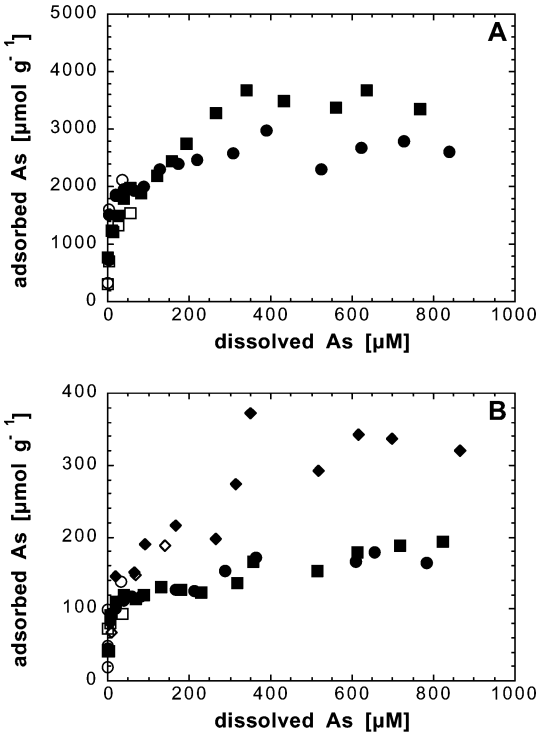

FIGURE 5. Arsenic sorption isotherms for (a) HFO and (b) goethite and magnetite. Symbols: (squares) As(V), (circles) As(III) with HFO and goethite, (diamonds) As(III) with magnetite. The open symbols are data from Figures 1 and 2. Experimental conditions: 0.01 M $NaClO_4$; 0.03 g L^{-1} HFO or 0.5 g L^{-1} goethite or magnetite, pH 4.0 for As(V) isotherms and pH 8.0 for As(III) isotherms.

sorption densities at most pH values (Figure 2c). The lack of agreement between data and model fits for magnetite and the difference in As(III) sorption edges observed between magnetite (mixed valence Fe-oxide) and Fe(III) oxides (Figure 2) may be due to differences in binding at Fe(II) and Fe(III) sites. Further spectroscopic analysis of arsenic sorption onto magnetite may help resolve some of these discrepancies.

Previous studies have also modeled As(V) and As(III) sorption onto iron oxides, using varying electrostatic models, surface species, and site densities for the iron oxides (Table 3). We examine the consistency of our results with those previously reported by using the surface species and constants in Table 2 to predict diagnostic features of the sorption edges. For As(V), at high As-to-Fe ratios (e.g., 100 μM total As(V) in Figure 1), a nearly linear decrease in sorption is observed with increasing pH. These sorption edges can thus be characterized in terms of two parameters, maximum sorption density (taken at pH 4, for consistency between studies) and the pH at which sorption density is reduced to half of its maximum value ($pH_{1/2max}$). The first of these parameters is less sensitive to the choice of surface species (and their surface complexation constants) and is largely a function of the site density. At lower As-to-Fe ratios, 100% sorption is observed over a broad pH range (e.g., 25 and 50 μM total As(V) in Figure 1), and the fit to these data sets is of little diagnostic value. For As(III), sorption behavior can be characterized in terms of a maximum sorption density that persists over a broad (circumneutral) pH range with decreasing sorption at both lower and higher pH. Since the model is poorly constrained at these extreme pH values, we define a single diagnostic parameter for As(III) sorption, the maximum sorption density (which can alternatively be expressed as the maximum %As(III) sorbed). When the concentration of total As(III) is less than that of the available sorption sites, the maximum sorption densities are most

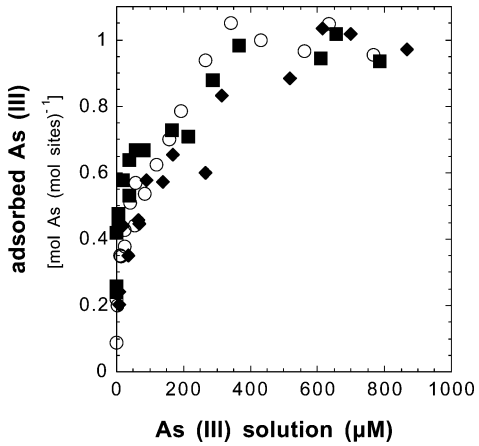

FIGURE 6. Normalized As(III) sorption isotherms: HFO (○), goethite (■), and magnetite (◆). Based on sorption data from Figure 5 normalized with respect to maximum sorption densities (Table 2). Experiments were conducted at pH 8.0 with 0.03 g L^{-1} HFO or 0.5 g L^{-1} goethite or magnetite.

sensitive to the values of surface complexation constants, rather than reflecting primarily the values of the site densities.

Comparison of our data sets with those listed in Table 3 illustrates the effect of differences in total As and Fe concentrations even at the same As-to-Fe ratios. For example, at an As-to-Fe ratio ($\times 10^{-3}$) of 9 (i.e., with 50 μM As(V)), we observe nearly 100% sorption onto goethite up to pH 7. At a similar As-to-Fe ratio but about 5-fold higher total concentrations, a nearly linear decrease in As(V) sorption was reported previously (*16*). This observed behavior is reasonably well predicted using the constants derived from our data set (Table 3). For both As(III) and As(V) sorption on goethite, the observed sorption density varies with total

concentrations at comparable As-to-Fe ratios. For example, at an As-to-Fe ratio ($\times 10^{-3}$) of 18, we observed maximum sorption densities of 145 and 125 μmol g^{-1} for As(V) and As(III), respectively, with 100 μM total As, whereas sorption densities of 200 and 215 μmol g^{-1} were previously reported for As(V) and As(III) with 1250 μM total As and an As-to-Fe ratio ($\times 10^{-3}$) of 22 (*21*). Again, our modeling results are in reasonable agreement with the previous observations (Table 3). Note, however, that for this data set, our model overpredicted the pH dependence of As(V) sorption on goethite.

With HFO, the As-to-Fe ratios ($\times 10^{-3}$) in our experiments ranged from 30 to 300, and our results can be compared with those of several previous studies (*17*, *18*, *20*, *23*). For As(V), our predictions are in moderate agreement with previous observations for As-to-Fe ratios ($\times 10^{-3}$) of 133 (*17*) and 210 (*23*), but for the ratio of 266 (*17*) the agreement is poor (Table 3). For As(III), good to moderate agreement of our predictions with previous observations is obtained for As-to-Fe ratios ($\times 10^{-3}$) of 27 (*17*, *20*), 53 (*23*), and 67 (*17*), but the agreement is poor for ratios of 133 and 266 (*17*). It should be noted that this lack of agreement reflects inconsistencies among data sets previously reported in an individual study (*17*). For both As(III) and As(V) sorption on HFO, the most pronounced discrepancies between our predictions and the previous observations are found for the As-to-Fe ratio ($\times 10^{-3}$) of 1189 (*18*). Under these conditions, the observed arsenic sorption exceeded the site density used in our model. Raven et al. (*18*) speculated that the high As(III) sorption density may have resulted from precipitation of a ferric arsenite phase. As further EXAFS and XRD analysis of the solids did not support the precipitation mechanism, Jain et al. (*46*) suggest that surface polymerization of ligand-bound As(III) may help explain their experimental observation.

Implications for Arsenic Mobilization. The sorption data presented in this study clearly show that the often-stated generalization that As(III) is more mobile in the environment than As(V) is too simplistic, when iron oxides are available as sorbents. The relative affinity of As(V) and As(III) depends on the solution composition (particularly pH) and characteristics of the iron oxides. In the pH range 6−9, typical of natural environments, As(III) is sorbed to a similar or greater extent than As(V) on HFO and goethite. This suggests that microbial reduction of arsenate would not necessarily increase its mobility. In a recent study of As- and Fe-enriched sediments, spectroscopic analysis of the sediment showed that As(V) reduction occurred in the uppermost sediment (0−2.5 cm), yet release of arsenic to the pore water occurred only deeper in the sediment coincident with iron mobilization (*47*). This suggests that reductive dissolution of the iron oxyhydroxide carrier phase and not just As(V) reduction is required to mobilize arsenic in these sediments.

The effect of competition for sorption sites is illustrated by phosphate. In the presence of phosphate, the crossover pH shifts to lower values. Thus, As(III) is sorbed preferentially to As(V) over a wider pH range in the presence of phosphate. However, below the crossover pH, phosphate depresses the sorption of As(III) more dramatically than that of As(V). Of course phosphate is not the only competing sorbate in the environment, and the properties of other sorbates must be considered in evaluating their effect on arsenic mobilization.

The intrinsic surface complexation constants for As(V) sorption are higher for goethite than for HFO (Table 2). Thus transformation of HFO to goethite would not decrease the affinity of the sorbed phase for As(V). In a recent laboratory study, aging of HFO (for 3000 h at pH 6 and 40 °C) did not result in desorption of As(V) (*30*). Indeed As(V) was found to be preferentially sorbed to the diagenetically altered iron oxide phases (*30*). Similarly, the binding strength of As(III) for the various iron oxides is comparable. Thus, again, transformation of HFO to goethite or magnetite would not decrease the affinity of the solid phase for As(III). However, the decrease in specific surface area and hence site density that accompanies transformation of amorphous iron oxides to more crystalline phases could increase the mobility of arsenic.

Acknowledgments

This work was partly supported by funding from the National Science Foundation (BES-0201888) and by the generous support of William Davidow. The constructive comments of two anonymous reviewers helped improve the manuscript.

Literature Cited

(1) United States Environmental Protection Agency, 40 CFR parts 9, 141, and 142, National Primary Drinking Water Regulations; Arsenic and Clarifications to Compliance and New Source Contaminant Monitoring; Proposed Rule. Washington, DC: Fed Regist 66: 20579−20584, 2001.
(2) WHO. *Guidelines for Drinking-water Quality. Volume 1: Recommendations*, 2nd ed.; WHO: Geneva, 1993.
(3) Chen, S. L.; Dzeng, S. R.; Yang, M. H.; Chiu, K. H.; Shieh, G. M.; Wai, C. M. *Environ. Sci. Technol.* **1994**, *28*, 877−881.
(4) Mandal, B. K.; Chowdhury, T. R.; Samanta, G.; Basu, G. K.; Chowdhury, P. P.; Chanda, C. R.; Lodh, D.; Karan, N. K.; Dhar, R. K.; Tamili, D. K.; Das, D.; Saha, K. C.; Chakraborti, D. *Curr. Sci. India* **1996**, *70*, 976−986.
(5) Thornton, I.; Farago, M. The Geochemistry of Arsenic. In *Arsenic Exposure and Health Effects;* Abernathy, C. O., Calderon, R. L., Chappell, W. R., Eds.; Chapman Hall: London, pp 1−16.
(6) Nickson, R. T.; McArthur, J. M.; Ravenscroft, P.; Burgess, W. G.; Ahmed, K. M. *Appl. Geochem.* **2000**, *15*, 403−413.
(7) Smedley P. L.; Kinniburgh D. G. *Appl. Geochem.* **2002**, *17*, 517−568.
(8) Masscheleyn, P. H.; Delaune, R. D.; Patrick, W. H., Jr. *J. Environ. Qual.* **1991**, *20*, 522−527.
(9) Macur, R. E.; Wheeler, J. T.; McDermott, T. E.; Inskeep, W. P. *Environ. Sci. Technol.* **2001**, *35*, 3676−3682.
(10) Cummings, D. E.; Caccavo, F., Jr.; Fendorf, S.; Rosenzweig, F. R. *Environ. Sci. Technol.* **1999**, *33*, 723−729.
(11) Ahmann, D.; Krumholz, L. R.; Hemond, H. F.; Lovely, D. R.; Morel, F. M. M. *Environ. Sci. Technol.* **1997**, *31*, 2923−2930.
(12) Hering, J. G.; Kneebone, P. E. In *Environmental Chemistry of Arsenic;* Frankenberger, W. T., Jr., Ed.; Marcel Dekker: 2001.
(13) Welch, A. H.; Westjohn, D. B.; Helsel, D. R.; Wanty R. B. *Ground Water* **2000**, *38*, 589−604.
(14) Ferguson, J. F.; Gavis J. *Water Res.* **1972**, *8*, 1259−1274.
(15) Bowell, R. J. *Appl. Geochem.* **1994**, *9*, 279−286.
(16) Manning, B. A.; Fendorf, S. E.; Goldberg, S. *Environ. Sci. Technol.* **1998**, *32*, 2383−2388.
(17) Pierce, M. L.; Moore, C. B. *Water Res.* **1982**, *16*, 1247.
(18) Raven, K. P.; Jain, A.; Loeppert, R. H. *Environ. Sci. Technol.* **1998**, *32*, 344−349.
(19) Goldberg, S.; Johnston, C. T. *J. Colloid Interface Sci.* **2001**, *234*, 204−216.
(20) Wilkie, J. A.; Hering, J. G. *Colloids Surf. A* **1996**, *107*, 97−110.
(21) Sun, X.; Doner, H. E. *Soil Sci* **1996**, *161*, 865−872.
(22) Appelo, C. A. J.; van der Weiden, M. J. J.; Tournassat, C.; Charlet, L. *Environ. Sci. Technol.* **2002**, *36*, 3096−3103.
(23) Swedlund, P. J.; Webster, J. G. *Water Res.* **1999**, *33*, 3413−3422.
(24) Manning, B. A.; Goldberg, S. *Soil Sci. Soc. Am. J.* **1996**, *60*, 121−131.
(25) Jain, A.; Loeppert, R. H. *J. Environ. Qual.* **2000**, *29*, 1422−1430.
(26) Gao, Y.; Mucci, A. *Geochim. Cosmochim. Acta* **2001**, *65*, 2361−2378.
(27) Zheng, Y.; van Geen, A.; Stute, M.; Dhar, R.; Mo, Z.; Cheng, Z.; Horneman, A.; Gavrieli, I.; Simpson, H. J.; Versteeg, R.; Steckler, M.; Goodbred, S.; Ahmed, K. M.; Shanewaj, M.; Shamsudduha, M. *Water Resour. Res.* Submitted for publication.
(28) Cornell, R. M.; Schwertmann, U. *The Fe Oxides: Structure, Properties, Reactions, Occurrences, and Uses*; VCH: Federal Republic of Germany, 1996.
(29) Ford, R. G.; Bertsch, P. M.; Farley, K. J. *Environ. Sci. Technol.* **1997**, *31*, 2028−2033.
(30) Ford, R. G. *Environ. Sci. Technol.* **2002**, *36*, 2459−2463.
(31) Roden, E. E.; Urrutia, M. M. *Geomicrobiol. J.* **2002**, *19*, 209−251.
(32) Fredrickson, J. K.; Zachara, J. M.; Kennedy, D. W.; Dong, H.; Onstott, T. C.; Hinman, N. W.; Li, S.-M. *Geochim. Cosmochim. Acta* **1998**, *62*, 3239−3257.

(33) Benner, S. G.; Hansel, C. M.; Wielinga, B. W.; Barber, T. M.; Fendorf, S. *Environ. Sci. Technol.* **2002**, *36*, 1705−1711.
(34) Schwertmann, U.; Cornell, R. M. *Iron Oxides in the Laboratory: Preparation and Characterization*; VCH: New York, 1991.
(35) Jolivet, J.-P.; Elisabeth, T. J. *J. Colloid Interface Sci.* **1988**, *125*, 688−701.
(36) Dzombak, D. A.; Morel, F. M. M. *Surface Complexation Modeling-Hydrous Ferric Oxide*; Wiley: New York, 1990.
(37) Schecher, W. D.; McAvoy, D. C. *MINEQL*$^{+}$, *V. 4.5*, Users Manual, Hallowell, ME, 1998.
(38) Liger, E.; Charlet, L.; Van Cappellen, P. *Geochim. Cosmochim. Acta* **1999**, *63*, 2939−2955.
(39) Marmier, N.; Delisée, A.; Fromage, F. *J. Colloid Interface Sci.* **1999**, *211*, 54−60.
(40) Herbelin, A. L.; Westall, J. C. *FITEQL4.0: A computer program for the determination of chemical equilibrium constants from experimental data*; Report 99-01; Oregon State University: Corvallis, OR, 1999.
(41) Liu, F.; De Cristofaro, A.; Violante, A. *Soil Sci.* **2001**, *166*, 197−208.
(42) Fuller, C. C.; Davis, J. A.; Waychunas, G. A. *Geochim. Cosmochim. Acta* **1993**, *57*, 2271−2282.
(43) Ferguson, J. F.; Anderson, M. A. Chemical forms of arsenic in water supplies and their removal. In *Chemistry of water supply, treatment, and distribution*; Rubin, A. J., Ed.; Ann Arbor Science: Ann Arbor, MI, 1974; pp 137−158.
(44) Mathur, S. S. Development of a Database for Ion Sorption on Goethite Using Surface Complexation Modeling. M.S. Thesis, Carnegie Mellon University, Pittsburgh, 1995.
(45) Sun, Z.-X.; Su, F.-W.; Forsling, W.; Samskog, P.-O. *J. Colloid Interface Sci.* **1998**, *197*, 151−159.
(46) Jain, A.; Raven, K. P.; Loeppert, R. H. *Environ. Sci. Technol.* **1999**, *33*, 3696.
(47) Kneebone, P. E.; O'Day, P. A.; Jones, N.; Hering, J. G. *Environ. Sci. Technol.* **2002**, *36*, 381−386.

Received for review January 9, 2003. Revised manuscript received June 27, 2003. Accepted July 3, 2003.

ES030309T